Locus: The Seton Hall Journal of Undergraduate Research

Volume 1 Article 9

October 2018

PANI and PEDOT:PSS Dip-Coating on CdS/CdTe Solar Cells

Michael Patullo

PANI and PEDOT:PSS Dip-Coating on CdS/CdTe Solar Cells

Michael Patullo
Supervisor: M. Alper Sahiner, Department of Physics, Seton Hall University
Department of Physics
Seton Hall University

Abstract

In an attempt to develop an advanced thin film solar cell high-conductive grade polyaniline (PANI) and poly(3,4-ethylenedioxythiophene)-poly(styrenesulfonate) (PEDOT:PSS) was dip-coated onto pulsed laser deposited (PLD) cadmium sulfide (CdS)/cadmium telluride (CdTe) semiconductor substrates. In previous studies, we have determined that applying these particular polymers and compounds on indium tin oxide (ITO) coated glass improves the photovoltaic conversion efficiency due to a reduction of the Schottky barrier resistance. In this study, we focus on optimizing the application of PANI and PEDOT:PSS by experimenting with dip-coating procedures and the solutions from which they are applied. An additional treatment of cadmium chloride that is traditionally highly regarded for increasing photovoltaic efficiencies was also applied to the surface of each cell. The thin films were characterized by scanning electron microscopy (SEM), energy dispersive x-ray spectroscopy (EDX), and ellipsometry techniques to verify and evaluate the successful application of their constituent materials. Electrical conductivity tests were also performed using a Keithley SourceMeter to determine photovoltaic efficiencies. Synthesis techniques, as well as structure, characterization, and efficiency results are discussed. It is also worth noting that the primary objective of this research was to produce the highest increase in solar cell efficiency possible, and not necessarily a solar cell with an impressive efficiency in of itself. Future research will involve additional SEM and EDX analysis to optimize the layers of each cell and help determine the homogeneity and elemental consistency of the polymer surface.

1. Introduction

The ever-increasing importance of solar energy in today's green initiative creates an immense demand for the continual improvement of photovoltaic technologies, particularly thin film solar cells. Over the last decade, the renewable energy sector has shown its potential to act as a substitute for traditional coal, natural gas, and petroleum sources. Photovoltaics alone have shown immense improvements in their material compositions which has since resulted in the reduction of their costs to just one-quarter what they were in 2010 [1]. In addition to declining prices, solar technologies have experienced an immense seven percent consumer growth improvement over that same period, an increase that is more than five times that every other renewable energy combined, as seen in Figure 1 [2]. Though photovoltaic efficiencies have increased significantly since the beginning of the century they do not operate near optimal conditions; even the most capable technologies only report a mere 46.0% of

their 68.2% theoretical values [3, 4]. Because of this, both prices and consumption rates will ultimately plateau if technological developments are not continually made. One study has even concluded that efficiency increases are directly proportional to price decreases [5]. All this being said, the photovoltaic field has reached a tipping point in which its expenses, demand, and efficiencies are primed to further the sector's advancement, but require a catalyst to do so. It is here that newer solar technologies are tasked with the responsibility of furthering the market's progress through the experimental testing of new methods of photovoltaic synthesis. Particular attention has been drawn to CdTe solar cells, a material that is widely considered one of the most promising thin film semiconductors, particularly when paired with CdS. Seeing a potential for significant scientific contribution, the Advanced Materials Synthesis and Characterization Laboratory at Seton Hall University has experimented with CdS/CdTe substrates in conjunction with high-conductive PANI and PEDOT:PSS back contacts.

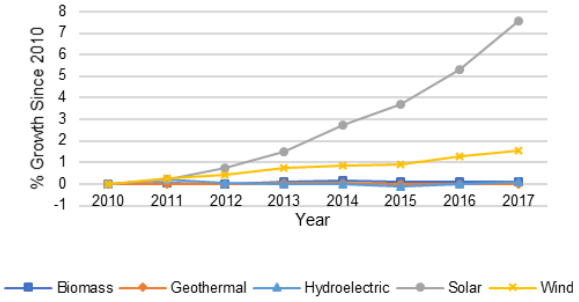

Figure 1. Solar market growth since 2010.

The application of n-type Cds and p-type CdTe onto an ITO conductive substrate creates a p-n junction between them in which current can flow freely in one direction but not in the other, effectively forming a diode. Free electrons within the CdS layer and free holes within the CdTe layer begin to pair at the junction and create a magnetic field over the depletion region with charges opposite those present within the semiconductors. During the photoelectric effect, photons strike the junction and eject electrons that generate a current from the positively charged CdTe to the negatively charged CdS. However, only photons with energies greater than that of the bandgaps of 1.49 eV and 2.42 eV for CdS and CdTe, respectively, will release valence electrons and ultimately contribute to their movement to the conduction band [6]. Traditional solar cells with metal back contacts used to complete their circuit only make it more challenging for an electron to travel across the bandgap due to the resistance present in the resultant Schottky barrier created at the semiconductor-metal junction [7]. Polymers like PANI and PEDOT:PSS serve as efficient back contact substitutes for these metals because of their organic nature, ease of application, lack of barrier resistance, high conductivity, and impressive work functions of approximately 5 eV each [6, 8].

2. Methods

To synthesize the glass/ITO/CdS/CdTe foundation of every cell, metals basis CdS and CdTe (Alfa Aesar, 99.999%) were separately ground to fine powders and hydraulically pressed under an applied load of 10,000 kg for 30 min into cylindrical targets 0.3175 cm high and 2.54 cm in diameter. Each target was then baked for 60 min at 350°C. Prefabricated square small 1.0 cm and large 2.54 cm glass/ITO substrates with a conductive thickness of 180 nm and sheet resistances of 9-15 Ω/sq and 8-10 Ω/sq, respectively (MTI Corporation) were prepared for CdS/CdTe application. Using a 248 nm ultraviolet krypton fluoride excimer laser (TuiLaser) beams of ultraviolet light were focused onto the targets at the conditions listed in Table 1 to form a plasma plume that thinly deposits the CdS and CdTe onto the glass/ITO substrates. Following the pulsed laser deposition, thickness measurements were taken on the newly applied CdS and CdTe layers using an LSE Stokes ellipsometer, the values of which were recorded for later analysis.

	CdS	CdTe
Duration	15 min	156 min
Energy	100 mJ	120 mJ
Frequency	10 Hz	12 Hz
Pressure	$6.7x10^{-4}$ Pa	$6.7x10^{-4}$ Pa
Temperature	200 °C	200 °C

Table 1. Pulsed laser deposition parameters.

In many studies treating thin film solar cells with cadmium chloride ($CdCl_2$) has been shown to significantly improve their efficiencies by approximately an entire order of magnitude [9]. In an effort to achieve similar results, a solution of anhydrous methyl alcohol (Macron Fine Chemicals) and anhydrous $CdCl_2$ (Alfa Aesar, 94%) was evaporated onto the CdTe surface for 15 min [6]. When $CdCl_2$ makes contact with CdTe the latter vaporizes and recrystallizes to improve its packing density, of which the chemical process is shown in Formula 1 [10]. Following the treatment, the solar cell was immersed in aqueous ammonium sulfide ($(NH_4)_2S$) (Alfa Aesar, 40-44% w/w) for 30 s, rinsed with distilled water, and baked at 400°C for 10 min [7]. The chemical composition of the $CdCl_2$ and $(NH_4)_2S$ allow for the creation of CdS, as demonstrated in Formula 2. Since the PLD technique is not guaranteed to create absolute uniform layers, the addition of new small particles of cadmium to the surface of the cell closes any pinholes and reduces CdS/CdTe lattice irregularities, helping prevent the cell from short-circuiting [6]. Following the $CdCl_2$ treatment, additional ellipsometer measurements were taken on the new layer which were again recorded for later analysis.

$$2Cd_{(g)} + Cl_{2(g)} + Te_{(g)} \rightarrow CdCl_{2(s)} + CdTe_{(s)} \quad (1)$$

$$CdCl_{2(s)} + (NH4)_2S_{(aq)} \rightarrow CdS_{(s)} + 2NH_4Cl_{(s)} \quad (2)$$

To form the back contact polymer layer, PANI, a neutral pH PEDOT:PSS (named PEDOT:PSS PH), and a surfactant-free PEDOT:PSS (named PEDOT:PSS SF) were mixed with various solvents to determine the solution with the best solubility. The powder emeraldine salt PANI (Sigma-Aldrich, 3-100 m) was mixed with dimethyl sulfoxide (DMSO) (Sigma-Aldrich, $\geq$99.7%) and anhydrous 1-Methyl-2-pyrrolidinone (NMP) (Sigma-Aldrich, 99.5%) in an effort to increase its base conductivity of 4 S/cm. The high-conductivity grade aqueous PEDOT:PSS PH and SF (Sigma-Aldrich, 1.1%) were mixed with ethanol (KOPTEC, 95%), ethylene glycol (EG) (Alfa Aesar, 99%), and DMSO again to increase their base conductivities of $<$1 S/cm as well [11]. Though the PANI was acquired as a readily infusible material, the aqueous PEDOT:PSS types had to be baked at 100°C for 1 hour in order to evaporate excess H_2O. After the PEDOT:PSS was isolated it was ground into fine particles and mixed with the appropriate materials. These particular solutions have been shown to increase polymer conductivity while simultaneously acting as effective solvents, with some studies reporting EG increases PEDOT:PSS conductivity by over 100 times, and DMSO by up to 1000 times [11, 12, 13, 14]. After 24 hours on a shaker with light heat, PANI showed the best results in NMP and the PEDOT:PSS types did similarly in DMSO. To also determine their ideal concentrations, 5, 10, and 15 mg/mL polymer solutions were made out of the top performing solvents [12]. After an additional 24 hour shake with heat, all three of the 15 mg/mL solutions showed the best-dissolved polymers and the smallest remaining particle sizes. Those three mixtures—15 mg/mL PANI in NMP, 15 mg/mL PEDOT:PSS PH in DMSO, and 15 mg/mL PEDOT:PSS SF in DMSO—were used throughout the remainder of the research. The structural formulas of those solutions are shown below in Figure 2.

To apply the polymers to the back contact of the cells, four of the small glass/ITO/CdS/CdTe samples numbered 922-925 were used to test the dipping speeds of 0.635, 1.27, 2.54, and 5.08 cm/min in a TL0.01 Dip Coater and their effects

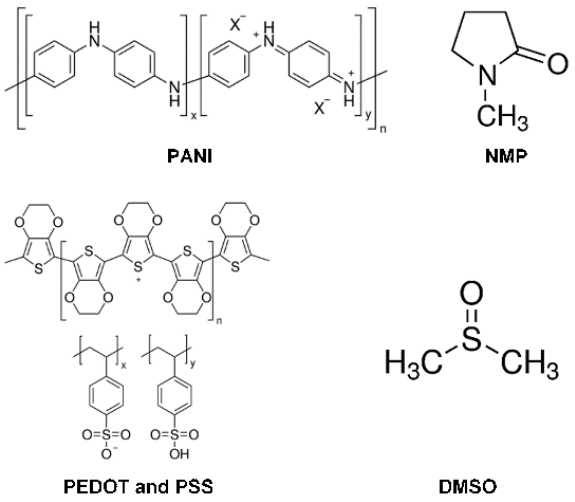

Figure 2. Chemical structure of polymer and solvent molecules.

on the resultant polymer characteristics. Sample 922 was dipped at 2.54 cm/min, 923 at 5.08 cm/min, 924 at 1.27 cm/min, and 925 at 0.635 cm/min. The dip-coating process involves completely immersing the cell within the desired solution and gradually removing it until the bottom surface of the sample breaks the plane of the top of the liquid. In the case of slower dips, cohesive forces between the molecules within the solution overpower the adhesive forces between it and the substrate, pulling more of the polymer off the cell back into the solution, resulting in a thinner back contact. Conversely, during faster dips the cell is removed too quickly for the cohesive forces to pull the polymer from its adhesion to the surface of the substrate, leaving a thicker back contact. The resultant surface is best described as a gel, having both the liquid properties of DMSO or NMP and the solid properties of the polymer chain network. Immediately following each dip the samples are baked at 75°C for 15 min to assist in the solidification of the back contact. The particular results of this procedure are documented in the upcoming sections, but the overall data showed that dipping at a rate of 1 in/min gave the best thickness measurements while preserving the overall uniformity of the polymer surface. Scaling this process up to the larger samples numbered 939 for PANI, 940 for PEDOT:PSS PH, and 941 for PEDOT:PSS SF showed similar results, a promising observation. The final set of ellipsometer measurements were taken on the polymer layers and were again recorded for later analysis.

An additional set of small samples numbered 935 for PANI, 936 for PEDOT:PSS PH, and 937 for PEDOT:PSS SF were submitted to visual analysis and chemical characterization using an SEM and EDX to verify the presence of the polymer back contact and its morphology. The images and elemental compositions of those results are discussed in the next sections. An additional 2.54 cm sample numbered 902 without a polymer to be used as the control and the large samples numbered 939-941 were submitted to electrical efficiency tests using a Keithley SourceMeter and a SoLux Solar Simulator light. These cells were wired at each corner as shown below in Figure 3. Flash-dry silver conductive paint (SPI Supplies) was used to make a small circular contact from which the solar cells were connected to the voltage source. The results of these efficiency tests and their current-voltage (I-V) plots are also discussed in the upcoming sections.

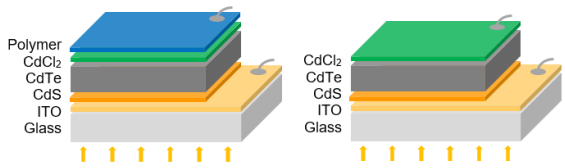

Figure 3. Layered cross-section of polymer (left) and control (right) cells.

3. Results

Perhaps the only thing more important than obtaining improved results in the sciences is that they are well founded. In order to verify that the ultimate solar cell efficiency results of this research are not obtained by chance, it is important to consider the many variables of thin film synthesis. Therefore, it is crucial that the ellipsometry,

SEM, and EDX results show only small variances so that the Keithley SourceMeter efficiencies can be considered independently strong results.

Ellipsometry measurements were taken at three different locations named points L, C, and R on each sample as illustrated below in to-scale Figure 4. The thickness of the small cells are displayed in Table 2, and the large cells in Table 3. Ideal measurements for each layer are approximately 200 nm of CdS, 1200 nm of CdTe, minimal amounts of $CdCl_2$, and 50 nm of polymer [6, 15]. Some studies suggest the optimal layer of a polymer back contact may even be as high as 70 nm [16]. The small sample data reports an average thickness of 196.35 nm of CdS, 1232.75 nm of CdTe, 22.54 nm of $CdCl_2$, and 14.5 nm of polymer with standard deviations of 0.23 nm, 0.21 nm, 0.66 nm, and 6.8 nm, respectively. Given their incredibly minute deviations, the CdS/CdTe deposited and $CdCl_2$ treated layers of this cell can be considered virtually identical and ideal for coating in a polymer. The large sample data reports an average thickness of 194.03 nm of CdS, 1216.41 nm of CdTe, 14.66 nm of CdCl2, and 18.3 nm of polymer with standard deviations of 8.12 nm, 41.37 nm, 1.37 nm, and 9.5 nm, respectively. It is also worth noting that the averages of control cell 902 are slightly different from that of the polymer-coated cells. The control reported an average of 179.99 nm of CdS, 1144.76 nm of CdTe, and 15.29 nm of $CdCl_2$, while the others averaged at 198.71 nm of CdS, 1240.29 nm of CdTe, and 14.45 nm of $CdCl_2$. Despite the seemingly large variation in these averages they only result in 9.9%, 8.0%, and 5.7% respective differences, which are somewhat high but nonetheless acceptable given the extent of the chaotic and unpredictable structure of each material after their deposition.

The surfaces of samples 935-937 were examined under an SEM and the images of their surfaces and cross-sections were acquired and labeled A and B, respectively. Figure 5 images display the PANI cell, Figure 6 images display the

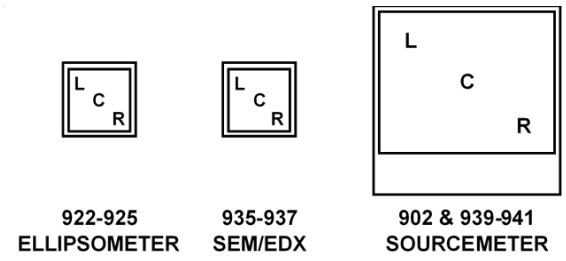

Figure 4. Ellipsometer positioning and corresponding sample testing numbers.

Sample	CdS	CdTe	$CdCl_2$	Polymer
922 L	196.20 nm	1233.29 nm	21.75 nm	23.2 nm
922 C	196.29 nm	1232.79 nm	22.98 nm	16.7 nm
922 R	196.29 nm	1232.64 nm	23.88 nm	16.7 nm
923 L	196.15 nm	1232.82 nm	21.71 nm	8.1 nm
923 C	195.97 nm	1232.78 nm	21.83 nm	9.5 nm
923 R	196.50 nm	1232.64 nm	22.70 nm	2.6 nm
924 L	196.79 nm	1232.86 nm	22.88 nm	17.0 nm
924 C	196.62 nm	1232.85 nm	22.81 nm	13.0 nm
924 R	196.62 nm	1232.68 nm	22.22 nm	25.6 nm
925 L	196.11 nm	1232.43 nm	22.68 nm	7.7 nm
925 C	196.27 nm	1232.60 nm	23.26 nm	10.6 nm
925 R	196.36 nm	1232.58 nm	21.77 nm	22.8 nm

Table 2. 1.0 cm sample ellipsometer results.

Sample	CdS	CdTe	$CdCl_2$	Polymer
902 L	179.82 nm	1144.03 nm	16.20 nm	N/A
902 C	180.78 nm	1145.59 nm	14.14 nm	N/A
902 R	179.38 nm	1144.67 nm	15.54 nm	N/A
939 L	199.71 nm	1239.48 nm	15.75 nm	7.1 nm
939 C	198.18 nm	1240.94 nm	15.26 nm	7.7 nm
939 R	199.23 nm	1239.82 nm	15.73 nm	1.7 nm
940 L	198.83 nm	1239.82 nm	15.50 nm	23.8 nm
940 C	198.80 nm	1241.38 nm	11.42 nm	24.6 nm
940 R	198.84 nm	1239.82 nm	12.56 nm	23.8 nm
941 L	198.85 nm	1239.89 nm	14.48 nm	30.9 nm
941 C	197.63 nm	1241.09 nm	14.13 nm	23.2 nm
941 R	198.28 nm	1240.37 nm	15.24 nm	21.8 nm

Table 3. 2.54 cm sample ellipsometer results.

PEDOT:PSS PH cell, and Figure 7 images display the PEDOT:PSS SF cell. During the PANI in NMP and PEDOT:PSS in DMSO dissolving process the polymers tend to form long chains while the solvent molecules attach at sites with free electrons. During the dipping procedure, the polymer and solvent gel assumes a fluid appearance, and after they are dried the polymers maintain their loosely structured network, which makes

them to a certain degree be visible in an electron beam generated image. Figure 5A shows a relatively uniform PANI surface with two $CdCl_2$ sites in the foreground, measuring approximately 2 m and 1 m across at their furthest points. In addition to verifying the success of the $CdCl_2$ treatment, the image shows that the PANI chains are either extremely dense to the point where their background is indistinguishable, or so scarce that they are hardly visible. Figure 5B displays a rather rough cross-section in comparison to its surface counterpart. As elaborated on in the upcoming EDX results the surface was confirmed to be PANI and not $CdCl_2$, which forces the consideration to be made as to why it appears so irregular. Since the SEM image captures a portion of the thickness of the cell as well as the back contact and since the PANI-NMP solution has an extremely low viscosity, it is probable that some PANI residue was left on the cross-section of the cell after drying. As a result, not only was the polymer coated onto the back contact but over the cross-section of the cell as well. Rough glass edges and directly opposing gravitational forces during drying are more than likely responsible for the surface abnormalities.

Figure 6A shows a rather obscure surface image of the PEDOT:PSS PH surface. Small applications of $CdCl_2$ are visible in several locations on the sample in addition to one larger area in the bottom right corner approximately 1 μm in diameter. The remainder of the image is both gray and black which suggests that the polymer forms a multidimensional surface on the back contact of the cell. Figure 6B displays a photograph very similar to that of the previous with layered polymer coatings and irregular surfaces. On the back of the cell and observable on the right side of the image there are isolated segments of excess polymer which are likely a result of minute oscillations in the pulley during the dip-coating process. Thickness inhomogeneity of the back contact is theoretically more common when using viscous solutions much like the PEDOT:PSS-DMSO mixture due to the fact that they can encounter complications during the drying process.

Figure 7A shows the most comprehensive back contact surface image with the PEDOT:PSS SF. Two patches of $CdCl_2$ can be seen, one of them measuring only a mere 0.1 μm. At a magnification of 8000x, though the molecules themselves are certainly not visible the general shapes from the networks they form are. In the image the dried polymer chain creates an effect with the solidified gel that is clearly visible, demonstrating a three-dimensional network effect in which the gray areas take up the foreground and darker layers constitute the background. Figure 7A suggests this sample may have the most effective back contact due to its continuous surface and visibly successful CdCl2 treatment. Its counterpart Figure 7B shows a rather smooth polymer surface, as seen on the right side of the cell. Slight discolorations between light and dark gray in the midsection of the width of the sample suggest that some of the PEDOT:PSS SF was present on the cross-section, which again is a less than ideal result. Like the image prior, smooth transitions between sample characteristics like color and topography suggest the corresponding large cell sample will show an improved efficiency. It should also be noted that the black arc on the left side of the image is not a crack in the sample but rather a zone of insufficient electron scattering, which can result in a dim capture.

An Oxford Inca x-Sight EDX was utilized in conjunction with the SEM to elementally characterize each of the images taken above. Since PANI and PEDOT:PSS are organic, the chemical structure of the back contacts of each solar cell should be primarily composed of carbon atoms with additional traces of hydrogen, oxygen, and nitrogen. Various points on the surface of samples 935-937 were tested and the results from each are displayed in Figure 8. Despite the uncertainties in the contents of its surface under the electron microscope as previously stated, the PANI cell shows clear organic results with nearly of its mass made of carbon and the remaining portion of

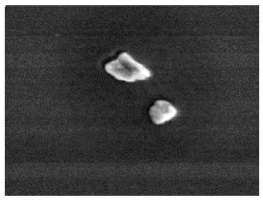

***Figure 5A** PANI surface*

***Figure 5B** PANI cross-section*

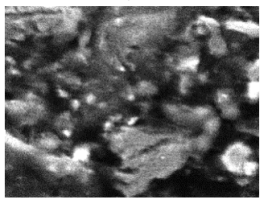

***Figure 6A** PEDOT:PSS PH surface*

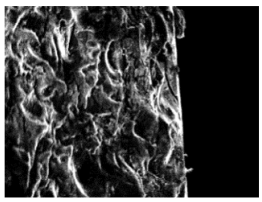

***Figure 6B** PEDOT:PSS PH cross-section*

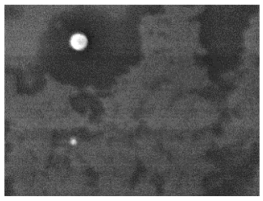

***Figure 7A** PEDOT:PSS SF surface*

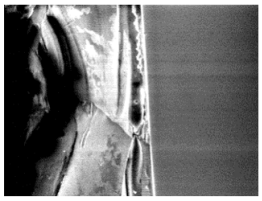

***Figure 7B** PEDOT:PSS SF cross-section*

oxygen. The PEDOT:PSS SF sample also reports similar findings, but with approximately 10% less carbon and an equivalent replacement of oxygen. These results are consistent with the chemical structure of those respective molecules, since the PANI network alone consists of approximately 80% molecular carbon weight, and the remaining oxygen content is accounted for with the addition of bonded and dried NMP. The PEDOT:PSS SF is no exception, with about 55% of its weight made of carbon—a value almost precisely that found by the EDX—and other large contributions of oxygen from the PEDOT chain, the PSS oligomer, and the solvent DMSO. While the PEDOT:PSS network does contain sulfur atoms in its heterocycles, the dissolving and dip-coating process should eliminate them from the final constituents of the back contact. This considered, the PEDOT:PSS PH results from the EDX clearly show that there are inconsistencies in the polymer layer, just as visually observed with the SEM. Nearly 15% of the molecular weight of the sampled area tested to be inorganic which strongly suggests that there were some complications during the dip-coating process, or that the CdCl2 treatment induced too much sulfur molecule migration to the back contact, making them detectable by the EDX [10].

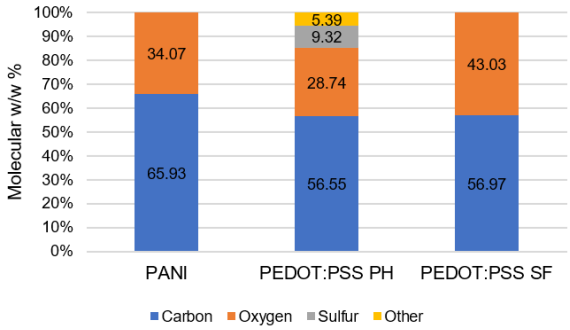

Figure 8. Energy dispersive x-ray spectroscopy of polymer samples.

Lastly, the efficiencies and I-V curves of the full-size samples numbered 902 and 939-941 were calculated and plotted using the Keithley SourceMeter and 100 mW/cm^2 SoLux Solar Simulator. Solar cell efficiency is calculated using the equation shown in Formula 3, where V_{OC} is the open circuit voltage, I_{SC} is the short circuit current, FF is the fill factor, P_{IN} is the input power, and η is the efficiency. The fill factor is the ratio of the optimized rectangular area beneath the I-V curve relative to that of a perfect cell, or for simplicity, the equivalent of the product of VOC and ISC, the x- and y-intercepts. To be thorough this breaks down into the equation listed as Formula 4, where V_{MAX} is the maximized voltage and I_{MAX} is the maximized current. Canceling identical terms and simplifying the product of I_{MAX} and V_{MAX} into P_{MAX}, the maximized power, leaves Formula 5 as expected. This being said, it is clear that the greater the fill factor of a cell is, the more likely it is to be of an improved efficiency. Other variables to consider include R_{SH}, the shunt resistance, and R_S, the series resistance. The former is the inverse of the slope of the curve at $V = 0$, and the latter is the inverse of the slope of the curve at $I = 0$. Larger R_{SH} values paired with smaller R_S values will lead to greater fill factors and greater efficiencies.

$$\eta = \frac{V_{OC} I_{SC} FF}{P_{IN}} \times 100\% \quad (3)$$

$$\eta = \frac{V_{OC} I_{SC}}{P_{IN}} \cdot \frac{V_{MAX} I_{MAX}}{V_{OC} I_{SC}} \times 100\% \quad (4)$$

$$\eta = \frac{P_{MAX}}{P_{IN}} \times 100\% \quad (5)$$

The results of the polymer back contact cells are plotted below in Figure 9, at which point it should be noted that the efficiency of the control cell was calculated to be $9.71\text{x}10^{-8}\%$. The PANI sample shows a weak curve and an efficiency of $1.16\text{x}10^{-4}\%$, while the PEDOT:PSS PH and SF report stronger efficiencies of $4.56\text{x}10^{-4}\%$ and $4.51\text{x}10^{-4}\%$, respectively. Ultimately these results show that the PANI contact improved the efficiency by nearly 1200 times, and the PEDOT:PSS types improved it by over 4600 times. Since the efficiencies of PEDOT:PSS PH and PEDOT:PSS SF are nearly identical, their curves almost entirely overlap. Small portions of the PEDOT:PSS PH curve are visible in orange from beneath the gray curve of PEDOT:PSS SF. Though the efficiency values themselves are important, the primary concern with this research was to verify whether or not organic back contacts would show any improvement, to which they did tremendously. These results and those before it are further elaborated upon in the upcoming section.

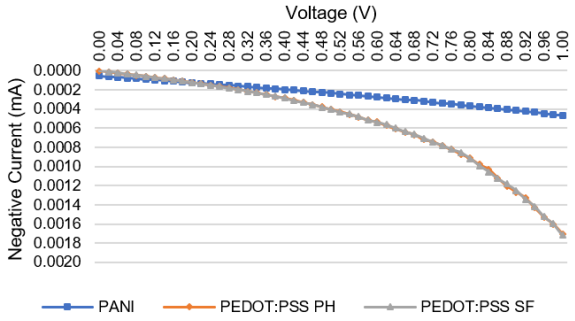

Figure 9. Keithley SourceMeter efficiencies of polymer samples.

4. Discussion

The results of this research can be divided into preliminary and secondary findings. Though data retrieved from the conductivity tests, the efficiency results of each cell, and whether or not certain polymers outperformed others are the stated objectives of this study, it is important that an analysis and consequential dialogue is given to the additional aspects of these experiments in order to promote the success of future research. Specifically, consideration—and to a certain extent, criticism—should be given to deposition techniques, the CdCl2 treatment, dip-coating procedure, and ellipsometer, SEM, EDX, and SourceMeter characterizations.

The primary function of the PLD process is to regulate the thickness of the CdS and CdTe layers by varying the conditions listed in Table 1, particularly the duration and frequency variables. The faster the laser pulses and the longer it runs the thicker the deposited layer will be. Again, the target thicknesses for CdS and CdTe were 200 nm and 1200 nm, respectively, while the acquired ITO substrate measured 180 nm. Many studies have been performed on the effect thin film p-n junction semiconductor thicknesses have on the ultimate efficiency of the cell, with one in particular identifying the optimal values of ITO/CdS/CdTe layers. It was concluded that the ideal thicknesses of the ITO and CdS were 100 nm each, while CdTe layers above 5000 nm trapped approximately 90% of incident photons and 15000-20000 nm trapped $\geq$99%, a value that inherently increases efficiency [18]. Though our experimental values are close to the optimal ones, they are certainly not the same. Instead, our specific thickness parameters are used in order to remain consistent with solar cells that the laboratory has synthesized in the past, in addition to the fact that they have been deemed sufficiently operative. This allows for a more precise determination as to whether or not newly synthesized cells are more or less efficient than their predecessors.

Out of every synthesis procedure, the $CdCl_2$ treatment is by far the most irregular due to the fact that evaporated materials are particularly difficult to control. It is not uncommon to have a thin film surface that is visibly more densely coated in $CdCl_2$ in some regions more than others. The duration, concentration, and chemicals themselves involved in the treatment work very well and are even backed by several similar publications [6, 7, 9, 10]. However, $CdCl_2$ can also be applied via close space sublimation, electrodeposition, screen printing, and sputtering. These processes will likely be considered for and incorporated into future research to determine which is most effective at increasing conductivity in organic polymer thin films. Even stronger consideration will be given to improving the existing technique by performing the treatment under vacuum to reduce irregularities in particle movement in an attempt to apply a more homogeneous $CdCl_2$ layer.

The PANI-NMP and PEDOT:PSS-DMSO solutions were tested in 5, 10, and 15 mg/mL concentrations, and it was determined that the latter contained the most uniform and dissolved particles. As a result, they were utilized for the back contact dip-coating procedure. These values are by no means optimal, however, and merely demonstrate that the ideal solutions consist of more polymer chains and fewer solvent molecules. Extensive research has been performed on both PANI and PEDOT:PSS to identify chemicals that simultaneously dissolve and increase polymer conductivity. Several studies have reported that the optimal concentration for DMSO in particular is approximately 2% v/v, while others have reported values up to 10% v/v [12, 13, 14]. Additionally, research with PANI has shown that every polymer concentration increase also results in efficiency increases [19]. These findings are consistent with our own, which of course directly impact those of the dip-coating procedure and the back contact thicknesses. In order to achieve the previously mentioned optimal thickness of 50 nm, future attempts will be made to reduce the time between coating and drying in order to preserve thickness and avoid polymer runoff.

Ellipsometry results showed relatively uniform CdS and CdTe surfaces, while some irregularities were evidently present in the $CdCl_2$ and polymer layers, the reasons for which were mentioned previously. When considering all measured samples, the average thicknesses for CdS was 195.19 nm, a 2.44% difference from the targeted value and 64.49% from the reported 100 nm optimal value. The average for CdTe was 1224.58 nm, 2.03% from the targeted value, 121.31% from the 5000 nm 90% photon trapping value, and 169.81% from the 15000 nm $\geq$99% photon trapping value. The average for all polymer layers was 14.08 nm, 112.07% from the 50 nm optimal value. Because the objective of this research is to identify and implement areas of thin film improvement rather than exclusively synthesize the most superiorly efficient cell, future research will likely include the utilization of atomic force microscopy (AFM) to obtain topographic data of the cell layers, particularly the polymer back contact. This technology will assist in the further optimization of dip-coating procedures by locating areas of uneven thicknesses and potential polymer absences.

Continued use of SEM and EDX techniques will be employed to verify the success of each deposition and dip-coat while simultaneously identifying the materials present on the sample. Attempts will be made as previously mentioned to improve these particular procedures in order to obtain a homogeneous layer at every junction, particularly the back contacts as seen in Figures 5-7. Ideal images would look very much like those of the PEDOT:PSS SF cell, with visible polymer chains, $CdCl_2$ sites on the surface, and a nearly uniform surface on the right side—the back contact—of the cross-section. Optimal EDX results would show that the back contacts consist exclusively of carbon and oxygen without the presence of sulfur or other impurities.

The conductivity results showed that the most efficient polymer back contact was the

PEDOT:PSS PH at $4.56x10^{-4}\%$, followed by PEDOT:PSS SF at $4.51x10^{-4}\%$, and PANI at $1.16x10^{-4}\%$. The control displayed an efficiency of $9.71x10^{-8}\%$, making the PEDOT:PSS types 4600x and the PANI nearly 1200x more efficient than the control. The experimental curiosity of the difference between the neutral, surfactant inclusive PEDOT:PSS PH and the acidic, surfactant-free PEDOT:PSS SF showed no variance. Both PEDOT:PSS types were calculated to have virtually identical efficiencies with a difference of just 1.1%, which shows that the acidity and presence of a surfactant had no impact on solar cell efficiency. These conclusions are generally concurrent with research performed by other individuals that show that PANI and PEDOT:PSS have an immense potential to increase solar cell efficiency by acting as back contacts in order to eliminate the Schottky barrier resistance.

5. Conclusion

CdS/CdTe solar cells are widely considered some of the most promising compounds in photovoltaic technology. The overall cost-effectiveness and versatility of these thin films are greatly superior to their traditional silicon counterparts. This research shows that dip-coating is an effective method for depositing conductive polymers on thin film solar cells. Due to the reduction of the Schottky barrier resistance, both PANI and PEDOT:PSS polymers improved photovoltaic conversion efficiency with respect to the control sample, which does not have a conductive polymer on the surface. Though the efficiency values recorded are low, the PANI and PEDOT:PSS electrodes prepared by dip-coating procedures were proven to be very effective. PEDOT:PSS in particular was shown to be very productive in increasing the thin film solar cell's efficiency. In future research, high-resolution AFM and SEM surface imaging paired with EDX characterization will help further control the dip-coating process in order to apply a more homogeneous and efficient polymer back contact.

Acknowledgements

The author would like to acknowledge Quinn Szanyi and Nnamdi Ene for their research contributions, William Cockerell, Olivia Rodgers, and the remaining members of the Advanced Materials Synthesis and Characterization Laboratory for their insight, the New Jersey Space Grant Consortium for its undergraduate fellowship, and the NSF-DMR 0420952 and TUBITAK-2221 grants for their funding. They would also like to especially recognize Dr. M. Alper Sahiner, whose unparalleled guidance and leadership made this research possible.

References

[1] Fu, R., Feldman, D., Margolis, R., Woodhouse, M., & Ardani, K. (2017). U.S. Solar Photovoltaic System Cost Benchmark: Q1 2017. National Renewable Energy Laboratory.

[2] U.S. Energy Information Administration. (2018). [Primary Energy Consumption by Source]. Unpublished raw data.

[3] De Vos, A. (1980). Detailed balance limit of the efficiency of tandem solar cells. *Journal of Physics D: Applied Physics*, 13, 839-846.

[4] Parrott, J. E. (1979). The limiting efficiency of an edge-illuminated multigap solar cell. *Journal of Physics D: Applied Physics*, 12(3), 441-450.

[5] Pillai, U. (2015). Drivers of cost reduction in solar photovoltaics. *Energy Economics*, 50, 286-293.

[6] Jarkov, A., Bereznev, S., Laes, K., Volobujeva, O., Traksmaa, R., Öpik, A., & Mellikov, E. (2011). Conductive polymer PEDOT:PSS

back contact for CdTe solar cell. *Thin Solid Films*, 519(21), 7449-7452.

[7] Josell, D., Debnath, R., Ha, J. Y., Guyer, J., Sahiner, M. A., Reehil, C. J., Manners, W. A., & Nguyen, N. V. (2014). Windowless CdSe/CdTe Solar Cells with Differentiated Back Contacts: J–V, EQE, and Photocurrent Mapping. *ACS Applied Materials & Interfaces*, 6(18), 15972-15979.

[8] West, R. M. (2013). Work Function Fluctuation Analysis of Polyaniline Films.

[9] Dharmadasa, I. M. (2014). Review of the CdCl2 Treatment Used in CdS/CdTe Thin Film Solar Cell Development and New Evidence towards Improved Understanding. *Coatings*, 4(2), 282-307.

[10] Kumar, S. G., & Rao, K. S. R. K. (2014). Physics and chemistry of CdTe/CdS thin film heterojunction photovoltaic devices: Fundamental and critical aspects. *Energy & Environmental Science*, 7(1), 45-102.

[11] Ouyang, J., Xu, Q., Chu, C., Yang, Y., Li, G., & Shinar, J. (2004). On the mechanism of conductivity enhancement in poly(3,4-ethylenedioxythiophene):poly(styrene sulfonate) film through solvent treatment. *Polymer*, 45(25), 8443-8450.

[12] Pathak, C. S., Singh, J. P., & Singh, R. (2015). Effect of dimethyl sulfoxide on the electrical properties of PEDOT:PSS/n-Si heterojunction diodes. *Current Applied Physics*, 15(4), 528-534.

[13] Deetuam, C., Weise, D., Samthong, C., Praserthdam, P., Baumann, R. R., & Somwangthanaroj, A. (2015). Electrical conductivity enhancement of spin-coated PEDOT:PSS thin film via dipping method in low concentration aqueous DMSO. *Journal of Applied Polymer Science*, 132(24).

[14] Hu, Z., Zhang, J., & Zhu, Y. (2014). Effects of solvent-treated PEDOT:PSS on organic photovoltaic devices. *Renewable Energy*, 62, 100-105.

[15] Khrypunov, G., Bereznev, S., Meriuts, A., Kopach, G., Kovtun, N., & Deyneko, N. (2010). Development Organic Back Contact for Thin-Film CdS/CdTe Solar Cell. P*hysics and Chemistry of Solid State*, 11(1), 248-251.

[16] Friedel, B., Keivanidis, P. E., Brenner, T. J. K., Abrusci, A., Mcneill, C. R., Friend, R. H., & Greenham, N. C. (2009). Effects of Layer Thickness and Annealing of PEDOT:PSS Layers in Organic Photodetectors. *Macromolecules*, 42(17), 6741-6747.

[17] Dharmadasa, I. M. (2014). Review of the $CdCl_2$ Treatment Used in CdS/CdTe Thin Film Solar Cell Development and New Evidence towards Improved Understanding. *Coatings*, 4(2), 282-307.

[18] Mohamed, H. A. (2015). Optimized conditions for the improvement of thin film CdS/CdTe solar cells. *Thin Solid Films*, 589, 72-78.

[19] Zheng, W., Angelopoulos, M., Epstein, A. J., & Macdiarmid, A. G. (1997). Concentration Dependence of Aggregation of Polyaniline in NMP Solution and Properties of Resulting Cast Films. *Macromolecules*, 30(24), 7634-7637.